

THERMAL AND STRUCTURAL BEHAVIOUR OF ORTHOTROPIC SLABS IN FIRE

XINMENG YU¹, ZHAOHUI HUANG², IAN W. BURGESS³ and ROGER J. PLANK⁴

ABSTRACT

When an orthotropic composite slab cast on steel decking is subjected to fire attack, there is a decreasing temperature gradient from the bottom surface to the top surface. In addition, the temperature within the continuous upper portion of the slab varies in the horizontal sense due to the presence of the ribs. This makes it different from a flat slab.

In this study, using a layered 9-noded iso-parametric slab element and a 3-noded beam element, an orthotropic slab element is developed to model orthotropic slabs in fire. The element is assembled from a solid slab element which represents the continuous upper portion of the profile, and a special beam element which represents the ribbed lower portion. An equivalent width for the cross-section of this beam element is determined according to the dimensions of the cross-section of the ribbed profile, and the beam shares the nodes of the solid slab element. Slight modifications are applied to the slab and beam models. The temperature within each layer of the slab element can vary between adjacent Gauss integration points so as to reflect the temperature gradients in the horizontal plane. It is reasonable to ignore the torsional resistance of the beam element, because it actually represents the equivalent of a group of ribs rather than one individual rib.

Two fire tests on composite slabs have been modelled to validate the approach. Cases of orthotropic slabs with wide range of parameters defining the ribbed profile have been studied, which show that the orthotropic slab model is robust and effective in reflecting the influence of the shape of ribs on the thermal and structural performance of the slabs in fire. The study shows the influence of decking shape on the temperature distribution in the slab.

¹ PhD Student, University of Sheffield, Department of Civil Engineering, S1 3JD, UK;
email: x.m.yu@sheffield.ac.uk

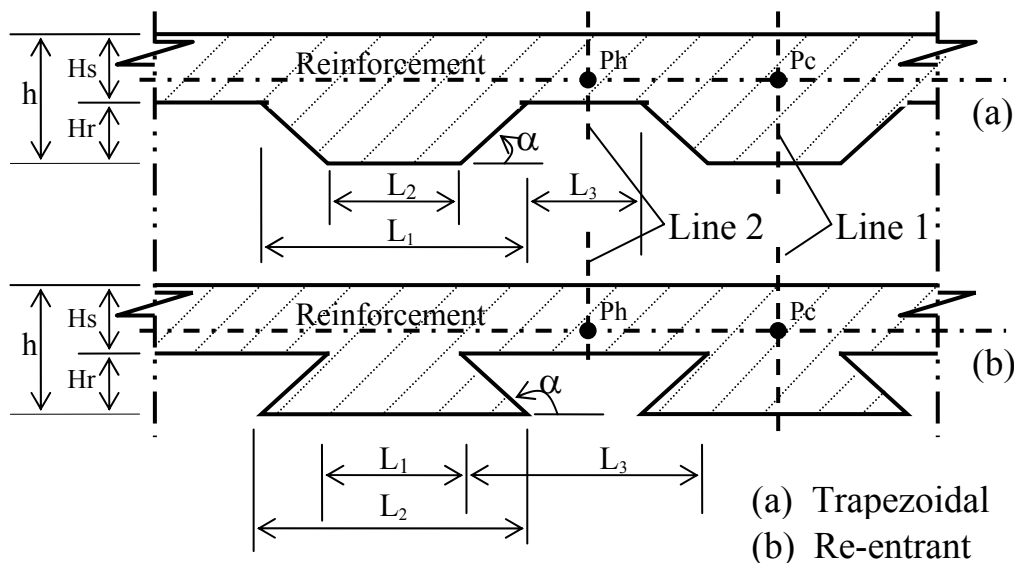
² Lecturer, University of Sheffield, Department of Civil Engineering, S1 3JD, UK;
email: z.huang@sheffield.ac.uk

³ Professor, University of Sheffield, Department of Civil Engineering, S1 3JD, UK;
email: ian.burgess@sheffield.ac.uk

⁴ Professor, University of Sheffield, School of Architecture, S10 2TN, UK;
email: r.j.plank@sheffield.ac.uk

NOTATION

Decking Geometric Parameters



Symbols

h	Slab depth	A45	$\alpha=45^\circ$; similarly for A90, A120, etc.
H_{eff}	Effective depth (defined in EC4)	P_h	Reinforcement position in the thinner parts of the slab
H_s	Concrete slab depth	P_c	Reinforcement position in the thicker parts of the slab
H_r	Height of steel decking (rib depth)	T_h	Temperature at P_h
L	Span	T_c	Temperature at P_c
L_0	Average of L_1 and L_2	T_{ec4}	Reinforcement temperature of an orthotropic slab at effective depth
L_1	Distance between two upper flanges	ϕ_{tf}	View factor at top flange of the decking
L_2	Width of the lower flange	ϕ_{web}	View factor at web of the web of the decking
L_3	Width of the upper flange		
RWR	Rib width ratio = $L_0/(L_1+L_3)$		
α	Angle between lower flange and web of decking		

1. INTRODUCTION

Orthotropic metal-decked composite slabs have been widely used in recent decades. These composite slabs consist of a cold-formed profiled thin-walled (typically, 0.6-1.2mm) steel decking, and concrete which is cast on top of this. Normally, the concrete is reinforced with a light anti-crack mesh, and may also contain individual bars, usually placed within the ribs. The profiles can be classified into trapezoidal and re-entrant types as shown above; trapezoidal decking may occasionally be used over long spans using extra-deep ribs which contain individual bars. However, the decking acts as a reinforcement, being bonded to the slab surface through indentations in the profile, and the composite slab itself has a very low centre of reinforcement compared to a conventionally reinforced slab. Due to the intrinsic efficiency of composite construction and the displacement of concrete by the profile shape,

considerably less concrete is used than in conventional reinforced concrete construction¹. Another advantage of an orthotropic slab over a flat one is that it saves construction time. Trapezoidal decking slabs are more popular than re-entrant ones because of ease of casting of concrete.

When the concrete is subjected to fire, the chemically bound water in the cement gel releases by dehydration into the liquid phase as free water, and the free water converts to the vapour phase. The water phase (solid, liquid or gaseous), the dimension of the structure, the mixture type, and the heating history all affect the temperatures in the slab in fire^{2,3}. Another complex feature comes from the coupled thermo-hydral-mechanical processes in the heated concrete. It is obvious that modelling of heat and mass transfer within concrete in fire is very complicated. Therefore, in this study, for simplicity, Huang's model⁴ is adopted to predict temperature distribution within the cross section of the composite slab. In this model, the thermal properties of concrete and steel are considered as temperature-dependent and the effects of moisture evaporation within the concrete are taken into account.

Thermal analyses show that, when an orthotropic slab is subjected to fire attack, the temperature within its continuous upper portion varies in the horizontal plane due to the presence of the ribs. The thinner part is subject to higher temperatures than the thicker part. The Cardington fire tests⁵ also show that the reinforcement temperature in the thinner portion is much higher than in the thicker portion. This issue should be taken into account in the development of orthotropic slab model to analyse ribbed slabs in fire.

In Eurocode 4⁶ (EC4), orthotropic slabs are treated as equivalent solid slabs with an effective depth (H_{eff}) and the steel decking is ignored in fire conditions. This method is not applicable to deep-deck slabs with rebar in the ribs. For these fire resistance is usually expressed in standard classes, ranging from 30 to 120 minutes (and beyond) in 30-minute intervals. Only exposure from below is considered, which in practical cases will always be decisive. These rules are highly empirical in nature, and lack a fundamental scientific basis⁷. As stated above, the presence of the rib makes orthotropic slabs different from flat ones in both thermal and structural behaviour.

A number of models have been developed for modelling of orthotropic composite slabs in fire. In the first phase of an ECSC research project⁷, a special-purpose model was developed for simulation of the mechanical behaviour of fire-exposed composite slabs. In order to obtain reasonable agreement between numerical and experimental results for the continuous decking slab, a full continuous horizontal crack separating the ribs from the concrete plane was assumed and explicitly taken into account. This was done simply by ignoring the contribution of the ribs and the steel decking to the stiffness.

Elghazouli and Izzuddin⁸ developed a model in which the composite slab was treated as an orthogonal elasto-plastic grillage of beam-column elements, and temperature variations were introduced across the two orthogonal cross-section directions as well as along the element length. The deflections were obtained from the integration of the orthogonal beam-column elements. The shortcoming of this model is that the realistic slab behaviour cannot be modelled properly in this way, since the effects of in-plane shear and Poisson's Ratio are ignored. Membrane action, which may cause a considerable reduction of displacements⁹ of slabs deforming in double-curvature due to two-way support conditions. Gillie *et al.*¹⁰ described a method of modelling composite floor slabs using a stress-resultant approach. A drawback of this method is that the model does not allow stresses to be output from the analysis.

In the University of Sheffield's software, *Vulcan*, an effective-stiffness model¹¹ was developed in which the orthotropic slab was treated as a solid slab with different orthogonal stiffnesses and layered temperatures which are uniformly distributed horizontally. The effective-stiffness factors obtained from cross-section bending stiffnesses at ambient

temperature are applied as constants to modify the material stiffness of the layered concrete slab throughout the fire stage. In fact, the effective-stiffness factors change at elevated temperatures, due to the degradation and failure of the materials. In Lim *et al.*'s model^{12,13}, the solid part of the ribbed slab was modelled as assembly of brick-like shell elements, and each individual rib was modelled using beam elements. It is obvious that a large number of elements are needed for modelling composite slabs of practical dimensions in this way, and computation is extremely expensive.

In this study a more robust procedure will be developed to model orthotropic slabs subject to fire conditions, taking into account more realistic temperature distributions.

2. NON-LINEAR PROCEDURE FOR MODELLING OF ORTHOTROPIC COMPOSITE SLABS

2.1 Orthotropic slab element

The software *Vulcan* has been developed at the University of Sheffield for three-dimensional analysis of composite and steel-framed buildings in fire. The program is based on a 3D non-linear finite element procedure in which a composite building is modelled as an assembly of beam-column, spring, shear connector and slab elements. The beam-column line element is three-noded, and its cross-section is divided into a matrix of segments to allow for variation of temperature, stress and strain through the cross-section¹⁴. Slabs are modelled using nine-noded layered plate elements based on Mindlin-Reissner theory, in which each layer can have different temperature and material properties⁹. Both material and geometric non-linearities are considered in beam-column and slab elements.

As shown in Fig. 1 the current orthotropic slab element is based on the previous beam and solid slab elements in *Vulcan*. The element is assembled from a solid slab element which represents the continuous upper portion of the profile and an equivalent special beam element which represents the ribbed lower portion. It is assumed that the reference axis of the beam element coincides with the mid-plane of the slab element. An equivalent width for the cross-section of this beam element is determined according to the cross-sectional dimensions of the ribbed slab, and it shares the 3 middle nodes of the solid slab element on the reference plane. The previous non-linear formulations of both the solid slab and beam elements are employed. The temperature of each layer of the slab element can vary between adjacent Gauss integration points. The cross-section of the beam element uses its segmented nature to represent different temperatures and materials within the ribs. In this model the beam element is used to represent a group of ribs of the composite slab, and hence the width of the beam element is an equivalent width calculated from the RWR and the width of the solid slab element. It is therefore reasonable to assume that the beam element has only uniaxial properties without torsional resistance.

The stiffness matrix of an orthotropic slab element \mathbf{K}_{orth} is assembled from the stiffness matrices of a nine-noded solid slab element \mathbf{K}_{slab} and a three-noded beam element \mathbf{K}_{beam} :

$$\mathbf{K}_{orth} = \mathbf{K}_{slab} + \mathbf{K}_{beam} \quad (1)$$

The internal forces of the orthotropic slab element \mathbf{F}_{orth} can be obtained from those of the solid slab element \mathbf{F}_{slab} and the equivalent beam element \mathbf{F}_{beam} as:

$$\mathbf{F}_{orth} = \mathbf{F}_{slab} + \mathbf{F}_{beam} \quad (2)$$

The detailed formulations of \mathbf{K}_{slab} , \mathbf{K}_{beam} , \mathbf{F}_{slab} , and \mathbf{F}_{beam} can be found in References 9 and 14.

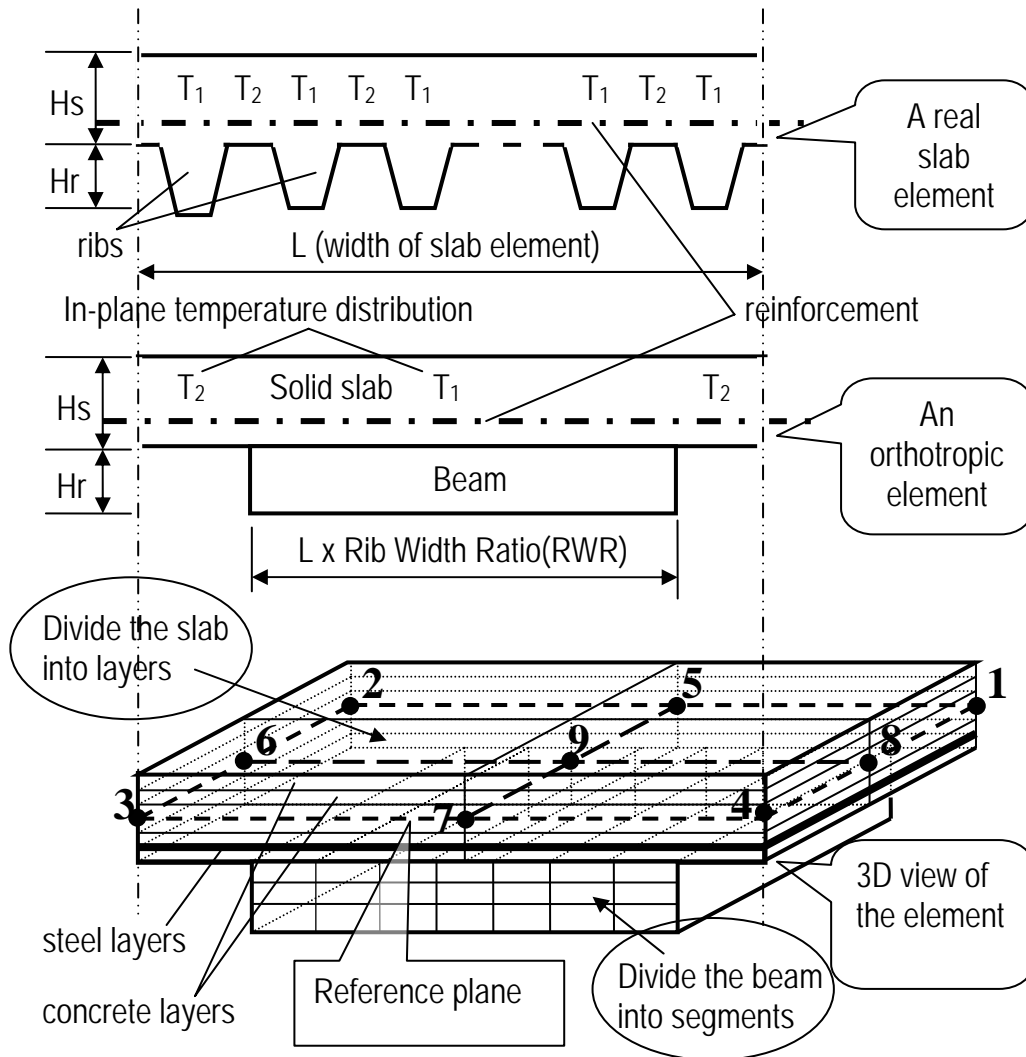


Fig. 1 - An orthotropic slab element model.

2.2 The simplified temperature distribution within each layer of the solid slab element

Due to the presence of the ribs, the temperature distribution within any layer of the solid slab element is non-uniform. In order to take into account this factor within the model a simplifying assumption was made; the temperatures within a layer are divided into three zones at the Gauss Integration Points (see Fig. 2). The higher temperatures at the axis of symmetry, Line 2, are applied to six Gauss Integration Points (1,2,3,7,8,9) and the cooler temperatures at the axis of symmetry, Line 1, are used for three Gauss Integration Points (4,5,6). The temperature distribution within the rib part at Line 2 is used to represent the temperature distribution of the cross-section of the beam element. This is a reasonable representation of the real temperature distribution within a ribbed slab. Hence, at each Gauss Integration Point, the material stiffness, strength, and thermal expansion is calculated according to the corresponding temperature.

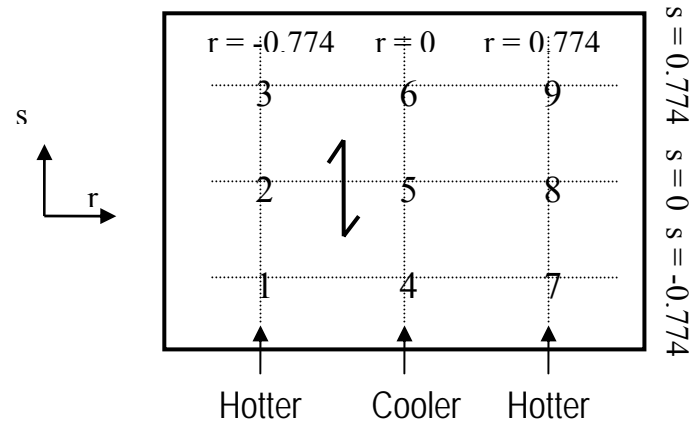


Fig. 2 – Temperature distribution at Gauss Integration Points within a layer of orthotropic slab element.

3. MODEL VALIDATION

3.1 Modelling of the TNO fire test

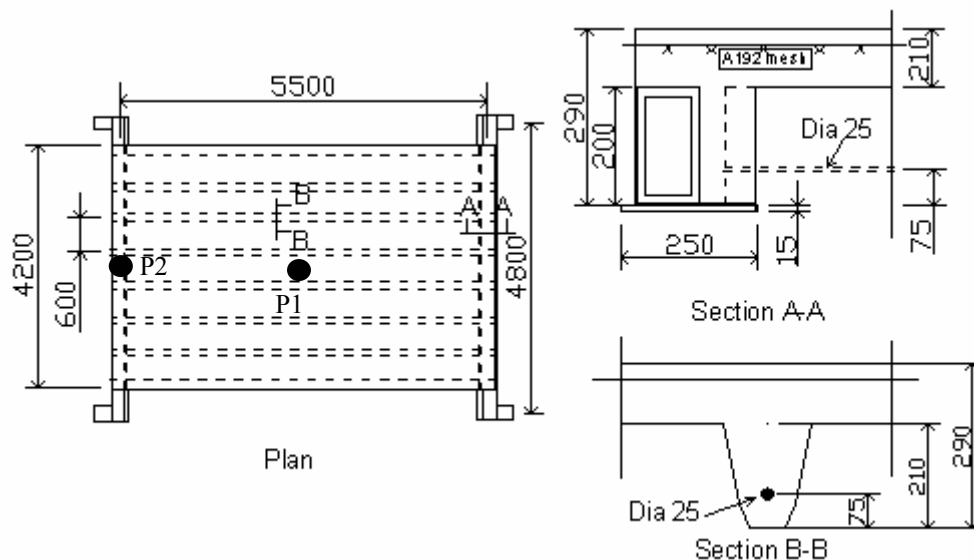


Fig. 3 - Details of TNO fire test.

A major fire test was carried out at TNO in the Netherlands in September 1996 as part of an ECSC research project¹. The specimen tested consisted of a single span of deep-deck normal-weight concrete slab with two RHS edge beams, simply supported at four corners. Fig. 3 shows the details of the test. The overall dimensions of the test specimen were 5.6m x 4.6m, with the edge beams spanning in the shorter direction. The overall depth of the slab was 290mm. The test load including self-weight was 6.65 kN/m^2 , a typical office building load intensity. The slab was unrestrained against thermal expansion, but the RHS edge beams were torsionally restrained at both ends. The edge beams were designed to achieve at least 60 minutes' fire resistance, and the composite slab was reinforced to achieve 120 minutes' fire resistance. In this numerical study, the tested material properties of structural steel, concrete and reinforcement were used. Further details are available from Reference 1. In order to

model the test, a thermal analysis was conducted to predict the temperature distributions within the cross-sections of the beams and ribbed slabs using *Vulcan*. The tested loads, and predicted temperature data were used in the structural modelling.

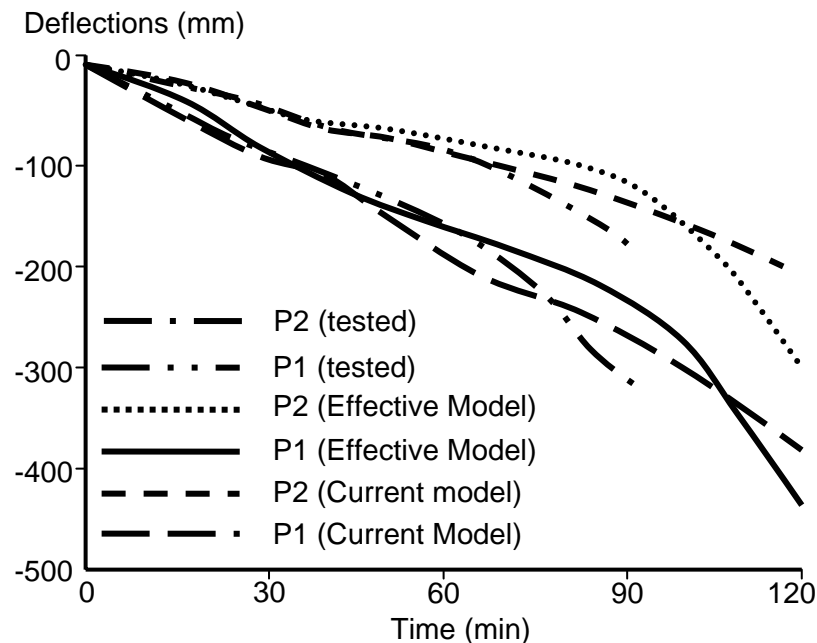


Fig. 4 - Comparison of predicted deflections with test results in TNO Fire Test.

Fig. 4 shows a comparison of predicted deflections using the current model and the previous effective-stiffness model at two key positions P1 and P2 (see Fig. 3), together with the test results. It can be seen that the curves predicted by the current model agree well with test results up to 70 minutes into the test. It is evident that the structural behaviour predicted by the two models differs.

3.2 Modelling the BRANZ fire test on a two-way simply supported decking slab

A series of full-scale fire tests conducted at the Cardington in the UK have shown that the fire resistance of unprotected composite floor structures is much better than standard furnace fire testing suggests. The composite concrete slabs may play an important role in increasing the fire resistance of the structure due to tensile membrane action, and so it is important to model the composite slabs correctly. Recently, six two-way simply supported concrete slabs were tested at the BRANZ fire test furnace in New Zealand. One of the tests, carried out on the 1st July 2002¹⁵, was on a Hibond orthotropic ribbed slab. The tested slab had the dimensions 4.3x3.3x0.130m, and was made of normal-weight concrete with 30MPa compressive strength. The slab was subject to a uniformly distributed live load of $3.0 \text{ kN} / \text{m}^2$ during the fire test.

The test was modelled as part of this study. The distribution of temperatures within the cross-section of the slab was predicted by *Vulcan*, and these temperatures were applied in the structural analysis.

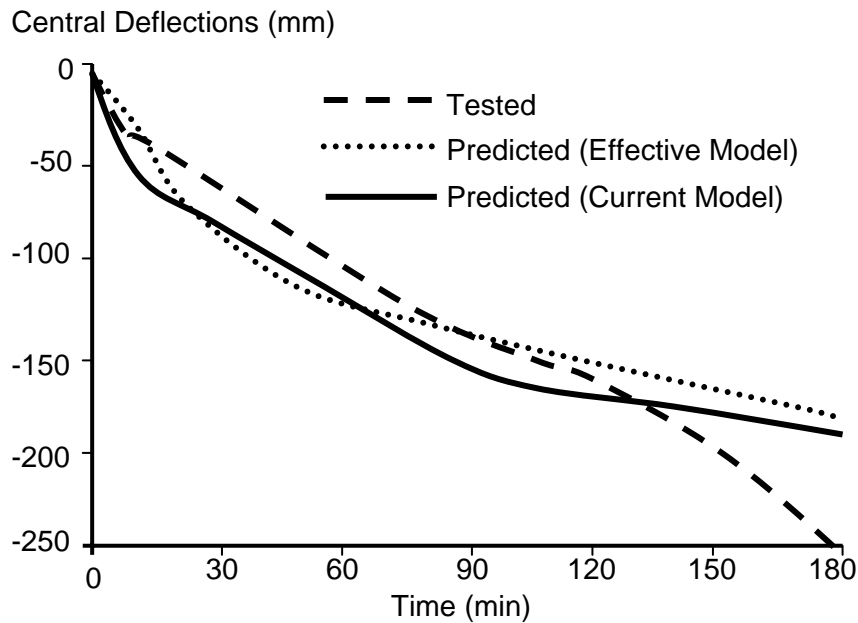


Fig. 5 – Comparison of predicted deflections with test results in BRANZ Fire Test.

Fig. 5 shows a comparison of central deflections predicted by the current orthotropic model and the effective stiffness model with test results. In the effective stiffness model the average temperature between the thinner and thicker parts was applied because the model assumed that each layer had uniform temperature distribution. Reasonable agreement was achieved by both models with the test results before 130 min test time. After that time the test deflections accelerated, but the predictions from both models were more stable. The reason for the difference between test and prediction may be due to the large cracks formed in the middle of test slab. The observations in the test¹⁵ support this: (a) Flames penetrated through the discrete crack in the middle of the slab in the later stage of the test; (b) Significant corner cracks formed during the test.

4. THE INFLUENCE OF RIB SHAPES OF ORTHOTROPIC SLABS IN FIRE

4.1 Decking shape parameters

Reference 7 lists a number of decking types with trapezoidal and re-entrant shapes. The different deckings were sorted and grouped according to the depth (H_r) and average width (L_0) dimensions of ribs. By considering the popularity and the rib width ratio (RWR) of existing deckings, the parameters of these groups were selected and are listed in Table 1.

While an orthotropic slab is subjected to fire, the fire radiation which acts on the bottom surface of the decking differs with shape and distance. The view factor is used to quantify this relationship. In this study, a simplified model was adopted to address this factor:

(1). Unit view factor was assumed at bottom of the rib, as the reference level.

(2). The view factors at the top flange (ϕ_{tr}) and web (ϕ_{web}) of the indented surfaces of the slab were assumed to be uniform and determined according to Fig. 6. This approximation was developed by Wickstrom *et al.*¹⁶ in 1990 and accepted by Eurocode 4².

Table 1: Orthotropic slab deckings used in the parametric study

Groups	L(mm)	L ₀ (mm)	H _s (mm)	RWR	$\alpha(^{\circ})$
--------	-------	---------------------	---------------------	-----	--------------------

					45	60	75	90	105	120
1	200	40	60	0.2	√	√	√	√		
2	200	60	40	0.3	√	√	√	√		
3	250	80	80	0.32	√	√	√	√		
4	200	120	40	0.6	√	√	√	√	√	√
5	200	120	60	0.6	√	√	√	√	√	√
6	250	175	60	0.7	√	√	√	√	√	√
7	300	210	40	0.7	√	√	√	√	√	√

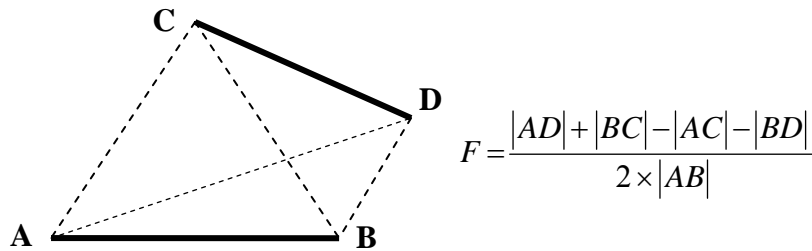


Fig. 6 – Determination of view factor, F , in 2-dimensional cases (radiation from $|CD|$ to $|AB|$).

4.2 Influences of shapes of decking on the thermal and structural behaviours

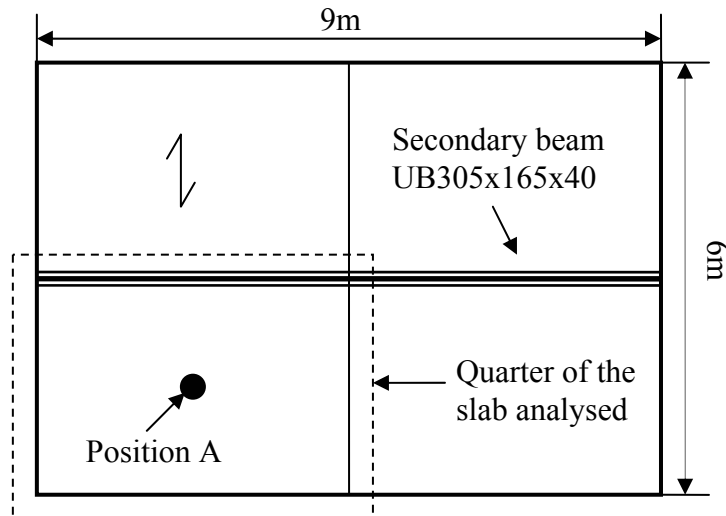


Fig. 7 – Two-way simply supported composite floor subject to ISO834 fire.

A two-way simply supported 9mx6m composite floor with a secondary beam in the middle of the shorter span (see Fig. 7) subject to an ISO834 fire was selected for this study. The secondary beam was assumed to be protected so that the bottom flange and web temperature linearly increased to 620°C at 180 minutes. Using the inherent symmetry only a quarter of the structure needed to be analysed. The thickness of the continuous thinner portion was 70mm. A142 mesh was located 20mm above the top flange of the decking. The uniformly distributed load was 5kN/mm². The compressive strengths of both the normal-weight concrete (NWC) and the light-weight concrete (LWC) at ambient temperature were 30N/mm². The study focused on the influence of the shape of the decking on the thermal and structural behaviour of the composite floor in fire.

The thermal analyses were conducted using *Vulcan*, again based on Huang's model⁴ and the structural behaviour was predicted by the new model. Eighty-six cases were modelled for both NWC and LWC in this study, including slabs treated as solid with nominal effective thicknesses obtained according to EC4.

Fig. 8 shows the temperature histories of the reinforcement in a typical group of profiled slabs (Group 6). Some general conclusions about the temperatures of reinforcement can be drawn from this study:

- For the slabs with $RWR \leq 0.32$ (Group1-3), the shape of the rib has little influence on T_h , but considerably influences T_c . The greater the angle α , the lower T_c becomes. Deeper ribs (with greater H_r) also affect the influence of the angle α on T_c . For those with RWR over 0.6 (Group 4-7) the shape of rib does not influence T_c very much, especially when α is greater than 90° , but decreases T_h by over 100°C .
- After 180min of the ISO834 fire, for NWC slabs T_h is in the range 650°C - 750°C and T_c in the range 450°C - 650°C ; for LWC slabs T_h is in the range 600°C - 700°C and T_c in the range 350°C - 650°C .
- If a profiled slab is treated as solid, with an effective thickness obtained according to EC4, the reinforcing mesh temperature is close to T_c . This gives the slab a better fire resistance than the real ribbed slab, especially in the later stages of the fire.

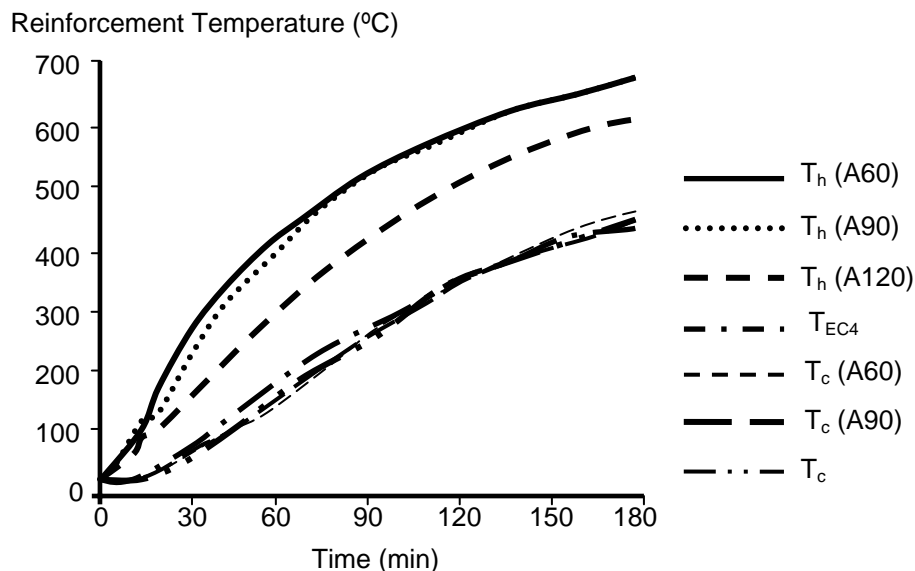


Fig. 8 - Reinforcement temperatures at thin and thick sections of the NWC slab (Group 6) in an ISO834 fire.

Fig. 9 shows the deflections at Position A (see Fig. 7) of the same group of profiled slabs. Some general conclusions concerning the structural behaviour of composite slabs in fire can be drawn, as follows:

- NWC slabs with $H_r \geq 80\text{mm}$ (Groups 3 and 7) or $RWR \geq 0.7$ (Groups 6 and 7) have better fire resistance than NWC slabs with $H_r < 80\text{mm}$ and $RWR \leq 0.6$ (Groups 1, 2, 4 and 5).
- LWC slabs have better fire performance compared to NWC slabs with the same compressive strength.
- Slabs with $\alpha = 90^\circ$ have higher deflection than those with other angles, for the same rib depth.

- For slabs with $RWR \geq 0.6$ (Groups 4-7), the shape has little influence on the deflection, except for those with $\alpha = 120^\circ$, which have the smallest deflection.
- Slabs with $H_r = 60\text{mm}$ show smaller deflection than those with H_r of 40mm and 80mm.
- For slabs with $RWR \leq 0.32$, there is a significant discrepancy in deflections between the orthotropic model and the equivalent solid slab with EC4 effective thickness.

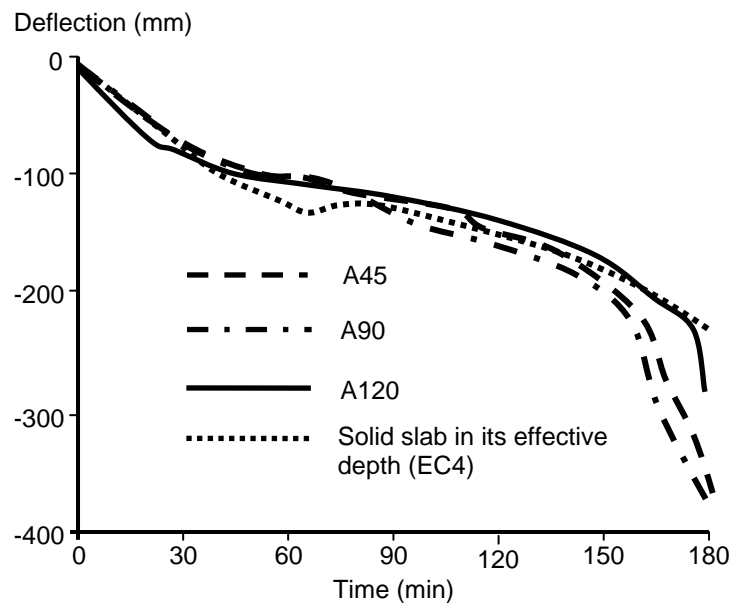


Fig. 9 – Deflections at Position A (see Fig. 6) of the NWC slab (Group 6) in the ISO834 fire.

5. CONCLUSIONS

In this paper the development of an orthotropic slab model to model ribbed slabs in fire has been described. The model is based on the slab and beam element formulations within the software *Vulcan* developed at the University of Sheffield. The two main new features of the model are:

- (1) The continuous top part of the ribbed slab is represented by solid slab elements, and the rib in the lower part is modelled as an equivalent beam element with uniaxial properties. Both the orthotropic character and membrane actions of ribbed slabs are taken into account in a logical manner. This approach also allows the modelling of deep-deck slabs.
- (2) The model allows non-uniform temperature distribution within each layer of the solid slab element. Hence, the temperature distribution across the cross-section of the profiled slabs can be represented more accurately. This overcomes the drawbacks of the previous effective-stiffness model, in which uniform average layer temperatures are used. In particular, better representation of reinforcement temperatures at the thin and thick sections of the cross-section of the ribbed slab is achieved by the current model.

A series of parametric studies using various decking shapes has been carried out. It shows that the current model can sensitively reflect the influence of shape on the thermal and structural behaviour. It also shows that the simplified method in EC4, which treats the orthotropic slab as an equivalent solid slab with an effective thickness, is not conservative when RWR is around 0.3, especially at the later stages of the fire; however for LWC slabs with $RWR \geq 0.6$, the agreement is very good. This discrepancy in performance mainly derives

from the thermal properties of concrete and the temperatures of the reinforcement, which are respectively hotter and cooler in the thinner and thicker portions of the slabs.

REFERENCES

- [1] *Corus Construction Centre* website: <http://www.corusconstruction.com>.
- [2] Bazant, Z.P. and Kaplan, M., “*Concrete at High Temperatures*”, ISBN 0-582-08626-4, Longman Group Limited, 1996.
- [3] Tenchev, R.T., Li, L.Y., Purkiss, J.A. and Khalafallah, B.H., “Finite element analysis of coupled heat and mass transfer in concrete when it is in a fire”, *Magazine of Concrete Research*, **53** (2), (2001) pp117-125.
- [4] Huang, Z., “*The Analysis of Thermal And Fire Performance of Cementitious Building Components*”, PhD thesis, University of Central Lancashire, 1995.
- [5] ECSC Project Report, “*Behaviour of a Multi-Storey Steel-Framed Building Subject to Natural Fires*”, Document Ref. : S423/2/Part T2, 1996.
- [6] Draft prEN1994-1-2: “*Eurocode 4 - Design of composite steel and concrete structures*”. Final Draft (Stage 34), 2003.
- [7] Both, C., “*The Fire Resistance of Composite Steel-Concrete Slabs*”, ISBN 90-407-1803-2-Y / CIP, Delft University Press, 1998.
- [8] Elghazouli, A.Y. and Izzuddin, B.A., “Analytical Assessment of the Structural Performance of Composite Floors Subject to Compartment Fires”, *Fire Safety Journal*, **36**, (2001) pp769-793.
- [9] Huang, Z., Burgess, I.W. and Plank, R.J., “Modelling Membrane Action of Concrete Slabs in Composite Buildings in Fire. Part I: Theoretical development”, *Journal of Structural Engineering, ASCE*, **129** (8), (2003) pp1093-1102.
- [10] Gillie, M., Usmani, A., Rotter, M. and O’Connor, M., “Modelling of Heated Composite Floor Slabs with Reference to the Cardington Experiments”, *Fire Safety Journal*, **36**, (2001) pp745-767.
- [11] Huang, Z., Burgess, I.W. and Plank, R.J., “Effective Stiffness Modelling of Composite Concrete Slabs in Fire”, *Engineering Structures*, **22**, (2000) pp. 1133-1144.
- [12] Lim, L.C.S., “*Membrane Action in Fire Exposed Concrete Floor Systems*”, PhD thesis, University of Canterbury, New Zealand, 2003.
- [13] Lim, L., Buchanan, A., Moss, P. and Franssen, J.M., “Numerical Modelling of Two-Way Reinforced Concrete Slabs in Fire”, *Engineering Structures*, **26**, (2004) pp1081-1091.
- [14] Huang, Z., Burgess, I.W. and Plank, R.J., “3D Modelling of Beam-Columns with General Cross-Sections in Fire”, *Paper S6-5, Third International Workshop on Structures in Fire, Ottawa, Canada*, pp323-334, 2004.
- [15] Lim, L.C.S. and Wade, C., “*Experimental Fire Tests of Two-Way Concrete Slabs*”, Fire Engineering Research Report 02/12, University of Canterbury, New Zealand, September 2002.
- [16] Wickström, U. and Sterner, E., “*TASEF-Temperature Analysis of Structures Exposed to Fire-User’s Manual*”, Swedish National Testing Institute, SP Report 1990:05.